

β -delayed fission from $^{256}\text{Es}^m$ and the level scheme of ^{256}Fm

H. L. Hall, K. E. Gregorich, R. A. Henderson, D. M. Lee, and D. C. Hoffman
Nuclear Science Division, Lawrence Berkeley Laboratory, Berkeley, California 94720

M. E. Bunker, M. M. Fowler, P. Lysaght, J. W. Starner, and J. B. Wilhelmy
Isotope and Nuclear Chemistry Division, Los Alamos National Laboratory, Los Alamos, New Mexico 87545
(Received 15 November 1988)

The 7.6-h isotope $^{256}\text{Es}^m$ was produced from a $2.5\text{-}\mu\text{g}/\text{cm}^2$ target of ^{254}Es by the (t,p) reaction. The reaction products were separated radiochemically, and the decay properties of $^{256}\text{Es}^m$ were determined via β - γ , γ - γ , and β -fission correlation techniques. From these measurements we were able to assign 57 γ rays to 26 levels in the daughter ^{256}Fm . An isomeric level was observed at 1425 keV and assigned a spin and parity of 7^- . This level has a $t_{1/2}$ of (70 ± 5) ns and we observed two β -delayed fissions with delay times in the proper time range to be associated with fission from this level. This gives a β -delayed fission probability of 2×10^{-5} for this level and a partial fission half-life of $0.8^{+8.9}_{-0.9}$ ms at the 95% confidence level.

I. INTRODUCTION

Beta-delayed fission (β DF) is a nuclear decay process in which a beta-decaying nucleus populates excited states in its daughter nucleus which then fission. These states can be above the fission barrier(s) of the daughter (yielding prompt fission), within the second well of the potential energy surface (a fission shape isomer), or within the first well of the potential energy surface. This decay mode was first postulated as a route for depleting the yield of heavy elements formed in supernovae in the seminal astrophysics paper by Burbidge, Burbidge, Fowler, and Hoyle.¹ β DF and the analogous electron-capture (EC) delayed fission (ϵ DF) have since become of interest for several additional reasons.

Measurements of the probability for β DF provide a sensitive probe of the structure of the fission barrier since the probability (and hence the half-life) of the fissioning level is exponentially dependent on the magnitude of the fission barrier. Appreciable β DF will occur only for neutron-rich nuclei sufficiently far from stability so that Q_β is comparable to the fission barrier of the daughter nucleus. From measurements of the relative probabilities for fission and γ emission from the level populated by β decay, the position of the level in the potential energy surface, i.e., relative to the fission barrier, can be determined. By measuring the lifetime of the fissioning level and the fission decay branch, a fission hindrance factor can be obtained.

β DF also allows the study of the fission of heavy nuclei from excited states, which can be used as a basis for predictions of fission properties of heavier nuclei. Since the liquid drop fission barrier rapidly diminishes with increasing Z^2/A in the heaviest elements, fission from excited states in these nuclei are strongly influenced by shell effects. Shell-stabilized fission barriers are also expected to govern the fission behavior of the superheavy elements.² Hence, β DF, by allowing investigation of the

fission barrier properties at non-ground-state energies in the heavy actinide region,^{3,4} can yield important data for comparison with theoretical predictions.

β DF also remains important in the astrophysical r process. This rapid neutron capture mechanism is believed to play a prominent role in stellar nucleosynthesis in supernovae.⁵ The β DF process is invoked to explain the observed isotopic abundances of the heavy elements and is offered as one reason why superheavy elements are not found in nature.⁶ A recent reexamination of data for heavy element yields from nuclear tests, however, has shown that the β DF process does not affect the mass yields of multiple neutron-capture products observed in these tests to the extent previously believed.^{7,8}

There have been only a few reports⁹⁻¹⁵ of experimental evidence for delayed fission processes. β DF has been reported to occur in $^{236,238}\text{Pa}$.⁹ The β -delayed fission probability P_{DF} , defined as the number of delayed fissions divided by the number of β decays of the parent

$$P_{\text{DF}} = \frac{N_{\beta f}}{N_\beta},$$

has been reported as about 10^{-10} for ^{236}Pa and 6×10^{-7} for ^{238}Pa .⁹ However, the latter value was not confirmed by a more recent study¹⁰ using automated chemical separation procedures in which β DF was not observed in ^{238}Pa . The upper limit for this decay mode was determined to be $P_{\text{DF}} \leq 2.6\times 10^{-8}$.

ϵ DF was reported in the region of Np and Am with mass numbers in the range 228-234 (Refs. 11 and 12) as early as 1966, but in those studies the fissioning species were not positively identified. More recently, ^{232}Am was reported to exhibit ϵ DF with a P_{DF} of $1.3^{+4}_{-0.8}\times 10^{-2}$.¹³ ^{242}Es has also been tentatively assigned an ϵ DF branch with $P_{\text{DF}} = (1.4\pm 0.8)\times 10^{-2}$.¹⁴ Lazarev *et al.*¹⁵ have reported the first observation of EC-delayed fission outside of the actinide series in the vicinity of ^{180}Hg .

One of the difficulties in studying delayed fission is obtaining nuclei sufficiently far from the line of β stability so that delayed fission becomes an observable phenomenon. As sources for studying delayed fission, supernovae and nuclear weapons tests suffer from intrinsic complexity, not only in the plethora of reactions occurring, but also in the difficulty of obtaining information about a single isotope's decay and the challenging task of recovering samples quickly enough to study short-lived isotopes. Isolation of a single element from an accelerator experiment is considerably quicker and easier. Thus, we have studied the decay of 7.6-h $^{256}\text{Es}^m$ to 2.63-h ^{256}Fm , produced via the $^{254}\text{Es}(t,p)^{256}\text{Es}^m$ reaction, exploiting radiochemical separation procedures to isolate einsteinium. Following chemical separation, the $^{256}\text{Es}^m$ decay to ^{256}Fm was studied using β - γ , γ - γ , and β -fission (β -F) correlation counting techniques, allowing us to explore the level structure of ^{256}Fm and to search for β DF.

In the experiment in which $^{256}\text{Es}^m$ was discovered,¹⁶ a level scheme for the ^{256}Fm daughter was proposed. This level scheme is shown in Fig. 1. In this level scheme, the β decay of $^{256}\text{Es}^m$ was primarily to the $K=7$ or 8 (1425-keV) level of ^{256}Fm . The 1425-keV level was then depopulated by γ decay to either the 8^+ or 6^+ level of the ground-state rotational band. We estimated the half-life of this highly forbidden $\Delta K=7$ or 8 transition to be in the few microseconds to few milliseconds range.

The fission half-life of ^{256}Fm at 1.4 MeV above the ground state was estimated¹⁷ to be $\sim 2.5 \mu\text{s}$ (assuming no hindrance from unpaired nucleons). If such were the case, then fission from the 1425-keV level should strongly compete with γ decay from this level. Even if the fission were hindered by unpaired nucleons involved in the

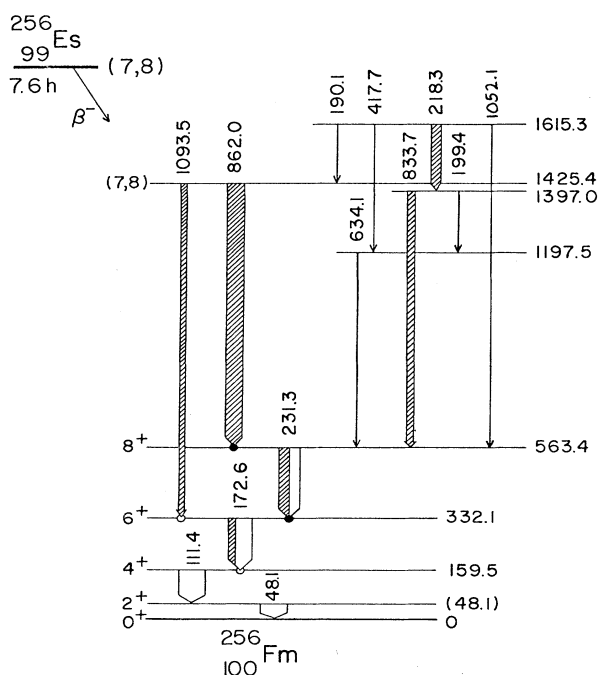


FIG. 1. Level scheme of ^{256}Fm proposed by Loughheed *et al.* (Ref. 16).

1425-keV level, we expected to be able to observe sufficient fission from this isomeric state to study both the total kinetic energy (TKE) and mass yield of fission from this excited level. Such information would give new insights into the fission decay properties of nuclei whose barriers are dominated by shell effects and thus further our understanding of the fission process.

II. EXPERIMENTAL

A. Target and irradiation

A source containing $\sim 0.1 \mu\text{g}$ of ^{254}Es ($t_{1/2}=276$ d) was chemically purified and electrodeposited in a 0.2-cm diameter circle on a 0.0125-mm thick palladium-coated beryllium foil. The deposited einsteinium was baked to ensure its conversion to the oxide form. The target thickness was determined by alpha spectroscopy to be $2.5 \mu\text{g}/\text{cm}^2$. The target was mounted in a target chamber illustrated schematically in Fig. 2. Cooling was provided on both sides of the target by a helium stream, but primarily on the upstream side of the target where there was a larger He flow.

Due to the high specific activity of the ^{254}Es target (about $2 \text{ mCi}/\mu\text{g}$), special safety precautions were taken during the course of the experiment. All cooling gas was passed through a HEPA filter after exiting the target chamber. An airborne alpha activity detector, or "sniffer," continuously monitored the air in the vicinity of the target chamber.

The tritium beam was provided by the Tandem Van de Graaff accelerator at the Ion Beam Facility (IBF) of the Los Alamos National Laboratory. The target was irradiated for about 7 h per bombardment with $6\text{--}10 \mu\text{A}$ of 16-MeV (on target) $^3\text{H}^+$. This energy corresponds to the peak of the excitation function for the production of $^{256}\text{Es}^m$, which was determined to be 16 mb in the discovery experiment.¹⁶ Recoiling products were caught on a gold catcher foil placed immediately downstream from the target as shown in Fig. 2. Following the irradiation

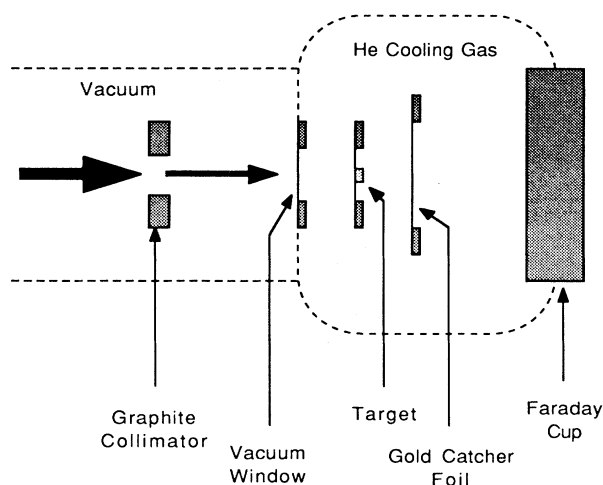


FIG. 2. Schematic representation of the target chamber used in these bombardments.

tion, the catcher foil and the target chamber were allowed to "cool" for approximately 1 h. This reduced the contribution of ^{256}Es ($t_{1/2}=25$ min) and allowed short-lived activities to decay. After the cooling period, the catcher foil was removed and einsteinium was chemically separated from other species produced. Thirteen irradiations and separations were conducted in a period of 5 d.

B. Chemical procedures

Upon removal, the catcher foil was taken to the chemistry laboratory at the Ion Beam Facility. The gold foil was removed from its mounting ring and dissolved with HCl-HNO_3 with a known amount of ^{241}Am ($t_{1/2}=432$ y) as a yield tracer. The resulting solution was then passed through a $2 \times 50\text{-mm}^2$ glass column packed with an anion exchange resin, Bio-Rad AG-1-X8 (200-400 mesh) which had been pretreated with concentrated HCl . The trivalent actinide and lanthanide activities were eluted with concentrated HCl , leaving the anionic gold complexes on the resin.

The effluent from the anion exchange column was evaporated to dryness and picked up in 0.1-M HCl . This solution was passed through a $2 \times 50\text{-mm}^2$ glass column

packed with a cation exchange resin, Bio-Rad AG MP-50 (200-400 mesh) in H_2O . Approximately $300 \mu\text{L}$ of 1-M NaCl was then passed through the column to remove ^{24}Na , which otherwise would be a significant source of background in the γ counting. The column was washed with 0.1-M HCl , and the actinides were separated as a group from the lanthanides by elution with concentrated HCl freshly saturated ($\sim 13\text{ M}$) with HCl gas. The resulting actinide fraction was then evaporated to dryness.

This actinide fraction was picked up in 0.1-M HCl and loaded onto another $2 \times 50\text{-mm}^2$ cation exchange resin column, this one packed with Hamilton AG-50W X-12 resin, size range $7\text{--}10 \mu\text{m}$. After loading, approximately $100 \mu\text{L}$ of H_2O and then $100\text{-}\mu\text{L}$ of 1-M NH_4Cl were passed through the column. The column was washed with H_2O , and the individual actinides were separated by elution with 0.5-M ammonium α -hydroxyisobutyrate (α -HIB) at $\text{pH } 3.71$.^{18,19} The einsteinium fraction was collected and dried. A flow chart of this chemical separation is shown in Fig. 3. This procedure took approximately 3 h to complete. At this point, the einsteinium was either taken immediately to the counting area for analysis, or was subjected to a second column separation as detailed below.

The einsteinium fraction from the α -HIB column still contained some fermium, primarily ^{256}Fm , which tailed into the einsteinium fraction and grew in from the decay of $^{256}\text{Es}^m$ during the relatively slow α -HIB column separation. This was not a problem for the coincidence

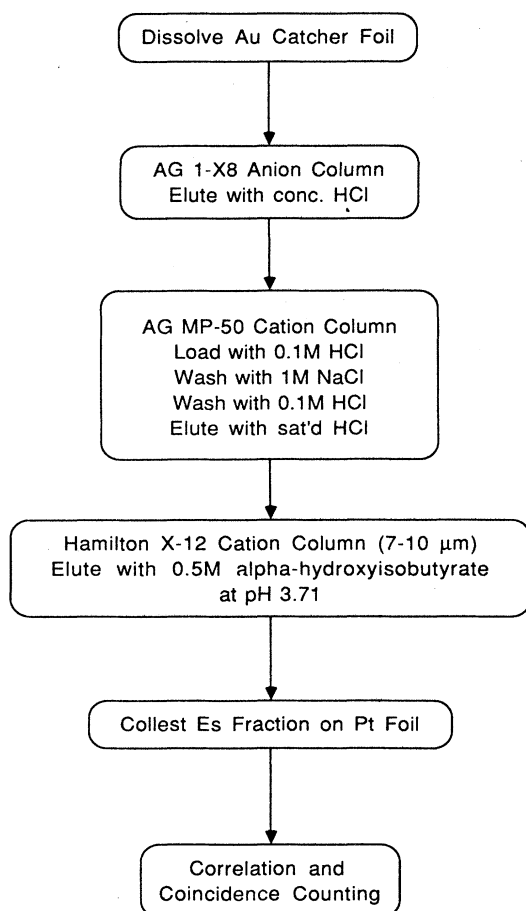


FIG. 3. Flow chart of the chemical separation procedure from the end of the bombardment to the end of the α -HIB column.

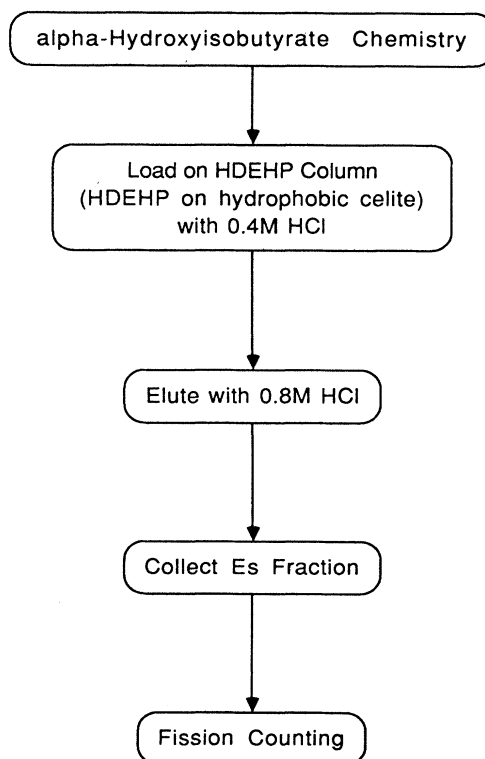


FIG. 4. Flow chart of the HDEHP separation procedure.

counting but did offer possible interference for our study of the growth of the ^{256}Fm spontaneous fission activity from the $^{256}\text{Es}^m$ parent. Extra purification would allow us to check for a possible long-lived βDF branch ($\geq 1\%$) from a level having a $t_{1/2}$ longer than could easily be measured using electronic timing coincidence techniques. If such a branch existed, the growth of the fission activity from the $^{256}\text{Es}^m$ would start from a nonzero activity at the time of separation. Therefore, it was necessary to prepare an einsteinium sample initially free of ^{256}Fm to determine if fissions were present after separation that could not be attributed to ^{256}Fm growth from $^{256}\text{Es}^m$. This extra purification was accomplished by processing the einsteinium sample from the α -HIB column through a reverse phase chromatographic separation.

This column was packed with hydrogen di(2-ethylhexyl) orthophosphoric acid (HDEHP) sorbed onto 50–75- μm particle size hydrophobic celite.^{20–22} The einsteinium sample was picked up and loaded onto the column using 0.4- M HNO_3 . $^{256}\text{Es}^m$ was then eluted away from ^{256}Fm using 0.8- M HNO_3 . A flow chart of this separation is presented in Fig. 4. This additional separation added about 45 min to the total separation time. The total time from the end of the bombardment to the start of counting was approximately 5 h.

C. Counting procedures

Following the chemical separation, the einsteinium sample was removed to the counting area and a variety of correlation counting measurements were performed. Information about the level scheme of the ^{256}Fm daughter was obtained by both β - γ and γ - γ counting, while information about the βDF behavior of $^{256}\text{Es}^m$ was obtained using β -F measurements.

For the γ - γ correlation counting, the sample was placed between two intrinsic germanium γ detectors at 180° with respect to each other. Each γ detector was able to serve as the start or stop signal for a time to amplitude converter (TAC). The resulting analog signals from the γ detectors and their affiliated TAC's were processed and stored using the Ion Beam Facility's computer system. This arrangement allowed real-time display of the incoming data and event by event storage on magnetic tape, thus permitting different software gates to be used in subsequent analysis. This increased flexibility was a significant improvement over the discovery experiment, and accounts for much of the improvement in the level scheme of ^{256}Fm .

For the β - γ correlation measurements, a 4-cm diameter plastic β detector provided the start signal to the

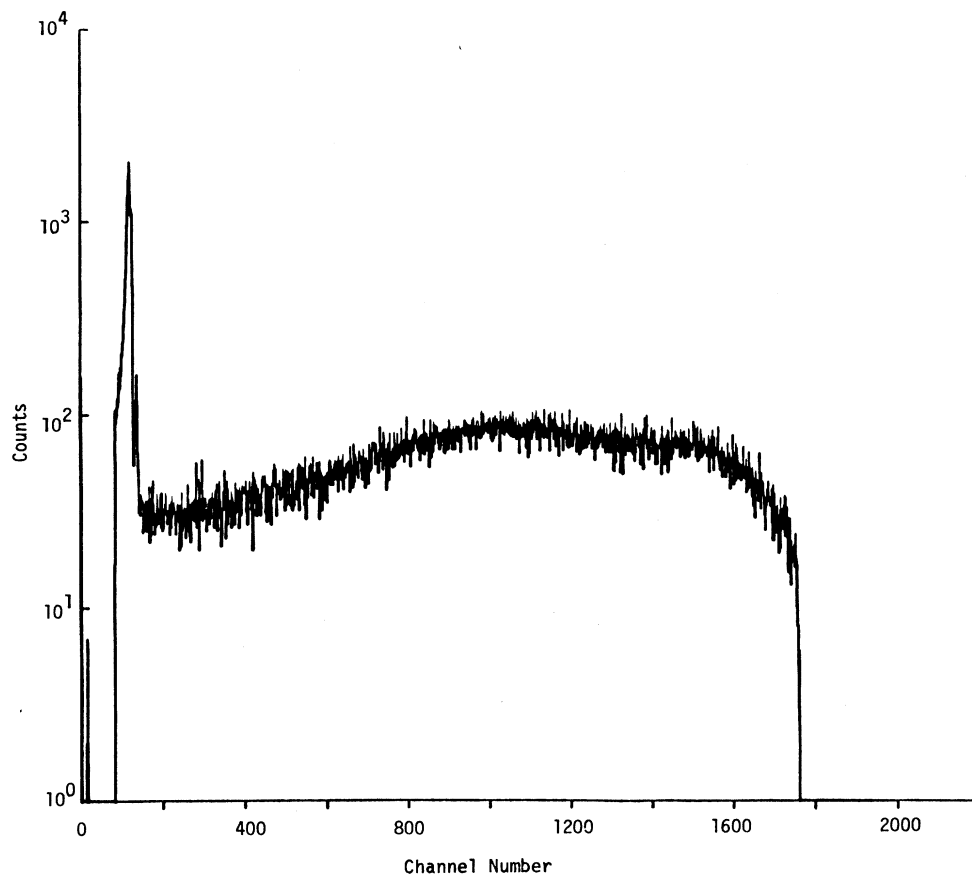


FIG. 5. α and fission singles spectrum obtained with the Si(Au) surface barrier detector in the β -F measurements with the detector at atmospheric pressure. The ^{256}Fm α particles form the narrow peak at about channel 275, while the fission fragments form the broad peak extending from the high end of the α peak to about channel 1750.

TAC. The stop signal was provided by an intrinsic germanium detector placed at 180° relative to the β detector. Again, the data were recorded using the on-site computer system.

For the β - F measurements, the same β detector used in the β - γ measurements provided the start signal for the TAC. The stop signal was provided by a 300-mm² Si(Au) surface barrier detector approximately 5 mm away from the sample. The surface barrier detector was operated at atmospheric pressure, which degraded its energy resolution, but not seriously enough to compromise its effectiveness in detecting fissions. Figure 5 shows a representative α and fission spectrum, illustrating that fission fragments could be distinguished from α particles.

III. RESULTS AND DISCUSSION

A. The $^{256}\text{Es}^m$ decay scheme

From the γ - γ -time correlation data, we were able to construct a more complete level scheme for ^{256}Fm than in the discovery experiment.¹⁶ This level scheme is shown in Fig. 6. From the γ - γ and β - γ data, we found evidence for six rotational bands with K^π values and bandhead energies of 0^+ (0 keV), 2^+ (682 keV), 2^- (881 keV), 3^+ (1100 keV), 5^+ (1252 keV), and 7^- (1425 keV). The energies and relative intensities of the γ rays observed in sin-

gles spectra are given in Table I. Other γ rays assigned to the $^{256}\text{Es}^m$ decay on the basis of γ - γ coincidence results are shown in Table II.

Representative γ -spectra are shown in Figs. 7 and 8. Energy calibration was obtained through the reported energies of fermium K x ray²³ and transitions accompanying the decay of ^{250}Bk , the daughter of ^{254}Es .²⁴

All of the $^{256}\text{Es}^m$ samples were of low intensity, resulting in poor counting statistics, especially in the γ - γ coincidence runs. Of the transitions shown in Table I, 26 have not been placed. However, these account for only about 10% of the total γ -ray intensity. The strongest unplaced γ ray is the 105.8-keV transition, which does not appear to be in strong coincidence with any other γ ray.

The intense 231-, 172-, and 111-keV transitions are in coincidence with each other and are assumed to depopulate, respectively, the 8^+ , 6^+ , and 4^+ members of the ground-state rotational band. The energies of these transitions imply a value of 48.3 keV for the energy of the 2^+ first excited state. The strong 861.8-keV γ ray is in coincidence with the 231.1-keV transition, indicating a level at 1425.5 keV which very likely has spin and parity 7^- based on its decay pattern. This level may be analogous to the 7^- state predicted by Soloviev and Siklos²⁵ to be the lowest-lying two-quasiparticle state in ^{254}Fm . The depopulation and half-life of this state are discussed in more detail in a subsequent section.

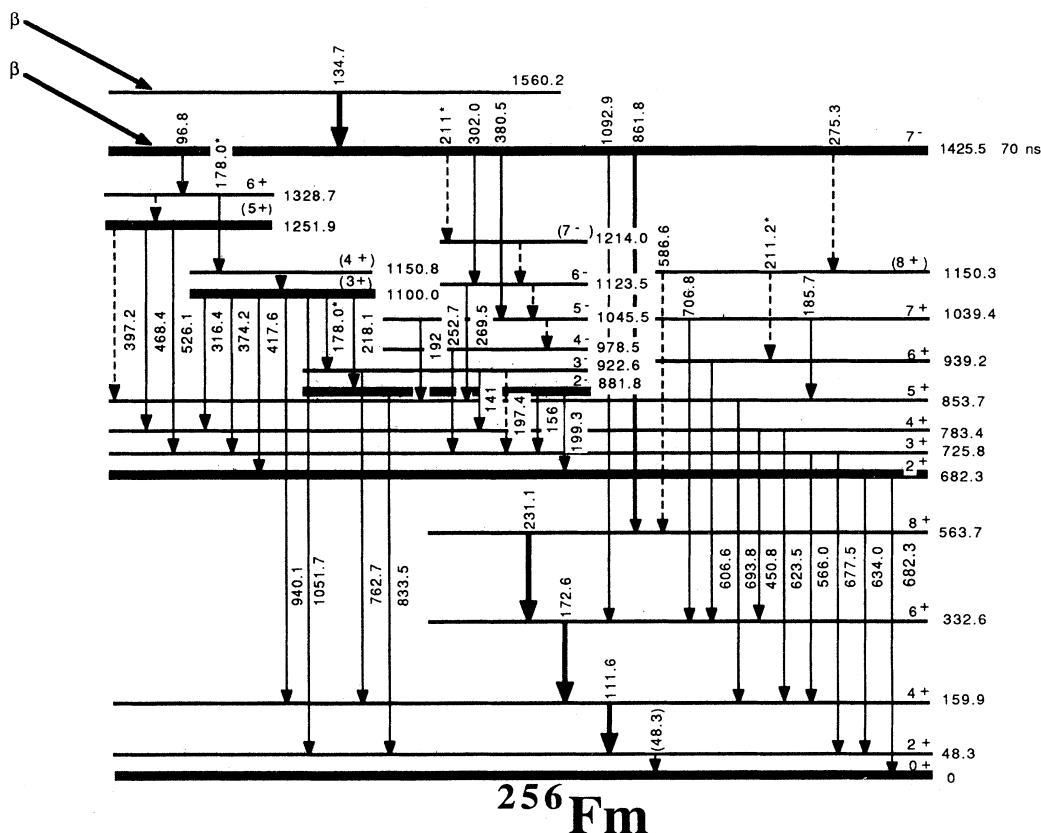


FIG. 6. Proposed level scheme for ^{256}Fm . Transitions placed in the scheme more than once are marked with an asterisk.

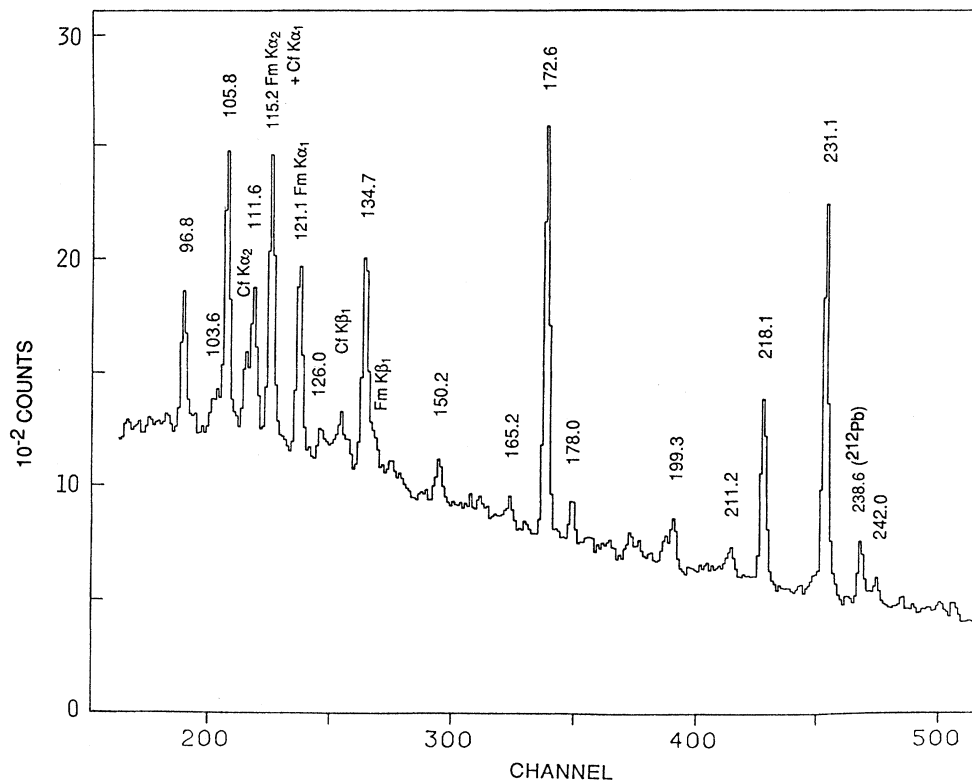


FIG. 7. Representative low-energy γ -ray spectrum from the decay of $^{256}\text{Es}^m$.

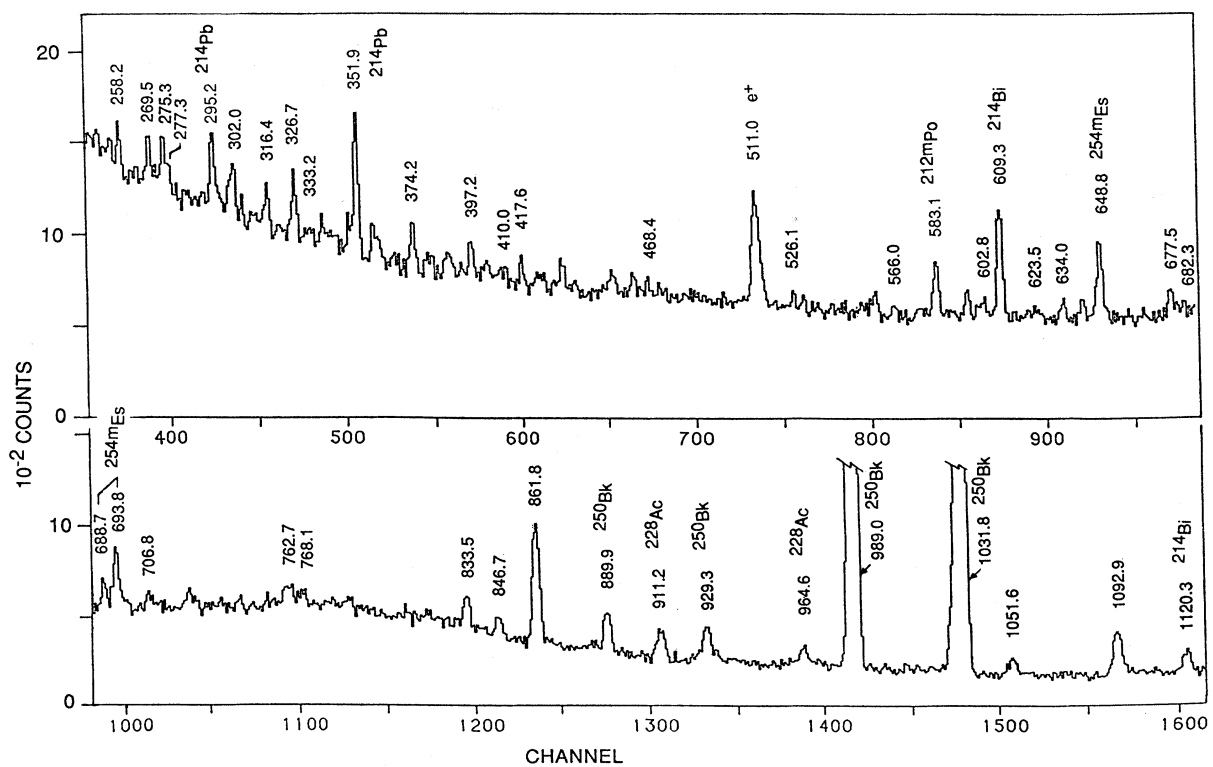


FIG. 8. $^{256}\text{Es}^m$ γ -ray spectrum from 250 to 1125 keV. Most of the unlabeled peak structures are either weak background lines or lines that did not decay with the $^{256}\text{Es}^m$ half-life.

TABLE I. Energies and relative intensities of γ -rays observed in the decay of $^{256}\text{Es}^m$.

Energy/keV ^a	I_γ ^b	Energy/keV ^a	I_γ ^b
96.8	2.55	275.3	1.15
103.6	0.80	277.3	0.60
105.8	5.12	297.5	0.52
111.6	2.79	302.0	0.82
126.0	0.71	316.4	1.02
134.7	5.12	326.7	1.37
150.2	1.16	333.2	0.36
158.9	0.31	343.0	0.49
165.2	0.50	374.2	1.43
172.6	9.70	380.0	0.38
178.0	1.10	397.2	0.74
181.5	0.28	410.0	0.38
185.7	0.25	417.6	1.53
190.1	0.55	468.4	0.90
197.4	0.79	526.1	0.82
199.3	1.40	566.0	0.50
211.2	0.87	602.8	0.77
218.1	5.69	623.5	1.12
229.0	0.65	634.0	1.73
231.1	12.00	677.5	2.21
232.7	0.58	682.3	1.84
240.3	0.36	706.8	1.15
242.0	0.79	762.7	2.28
247.4	0.38	768.1	2.25
252.7	0.25	833.5	5.45
255.3	0.55	846.7	2.02
258.2	0.65	861.8	19.66
264.1	0.38	1051.5	2.56
269.5	0.75	1092.9	9.24

^aFor transitions of intensity ≥ 1.0 , the energy uncertainty is ± 0.15 keV.

^bIntensity scale arbitrary.

The 682.3-keV level is the lowest intrinsic state observed and is assumed to be the 2^+ gamma vibrational state, which occurs in ^{254}Fm at 694 keV. The next highest intrinsic state occurs at 881.8 keV, which is assigned as 2^- since it decays only to the two lower-lying 2^+ states. This state is assumed to be a 2^- octopole state, analogous to the one predicted by Neergård and Vogel²⁶ to occur at ~ 800 keV in ^{254}Fm . The 881.8-keV

TABLE II. $^{256}\text{Es}^m$ γ -rays seen in coincidence measurements, but not resolved in single spectra.

E_γ /keV ^a	Relative I_γ ^b	γ -keV	Gate/keV
141	0.09	622	
192	0.12	696	
252	0.07	678	
156	0.08	678	
451	0.15	172	
587	0.2	231	
607	0.4	172	
694	0.8	111	
941	0.8	96	

^aEnergy uncertainties are typically ± 1.5 keV.

^bSame relative intensity scale as in Table I.

level is fed most strongly by the 218.1-keV transition. Intensity balance at the 881.8-keV level can only be achieved if the 218.1-keV transition is $E1$. Thus, the 1100-keV level is assigned positive parity, and from its observed branching to lower states, a spin of 3 is indicated.

The states at 1150, 1251, and 1328 keV are not as well established. The main clue to this portion of the scheme is that the 96.8-keV γ ray follows the 134.7-keV transition and is in coincidence with the 178-, 197-, 199-, 218-, 316-, 374-, 397-, 417-, 468-, 526-, 624-, 634-, 677-, 682-, 833-, and 1052-keV transitions. From intensity balance considerations, the 96.8-keV transition is almost certainly $E1$. Placing it as depopulating the 7^- level to a 6^+ level at 1328 keV, which is in turn depopulated by the 178-keV transition to the 4^+ member of the proposed 3^+ band, is consistent with the γ - γ results. The coincidence data and the energy difference of the 468- and 526-keV transitions strongly suggests that these transitions feed, respectively, the 4^+ and 3^+ members of the 2^+ band, establishing a state at 1251.9 keV, which is presumably fed from the 1328-keV level by an unobserved 77-keV transition. Since 77 keV is the approximate energy difference between the spin 5 and 6 members of rotational bands in this nucleus, we assume that the 1251-keV level is 5^+ .

Our proposed scheme accounts for only about one-third of the total intensity depopulating the 1100-keV level. There is a strong (150.2–218.1)-keV coincidence that could account for all of the missing intensity if the 150.2-keV transition were of $M1+E2$ multipolarity. However, the exact placement in the scheme of 150.2-keV transition is unclear. In this case, and in constructing other portions of the decay scheme, we were hampered by the lack of conversion-electron data, which not only would have revealed a number of highly-converted low-energy transitions, but would also have yielded information regarding transition multipolarity.

B. The 1425-keV level

From the β - γ data, the half-life of the 1425-keV level was determined to be 70 ± 5 ns, much shorter than we had anticipated from the earlier¹⁶ level scheme and the systematics of K -forbidden transitions.²⁷ A representative TAC spectrum for the 231-keV γ ray is shown in Fig. 9.

The 861.8- and 1092.9-keV $\Delta K=7$ transitions, which are responsible for about half of the depopulation of the 1425-keV level, are unusually fast K -forbidden $E1$ transitions. The Weisskopf hindrance factors, F_W , given by

$$F_W = \frac{(T_{1/2})_{\text{exp}}}{(T_{1/2})_{\text{theo}}}$$

for these two transitions are, respectively, 0.76×10^9 and 3.3×10^9 (based on our estimate of 57 for the total intensity of all transitions depopulating the 1425-keV level, using the intensity scale of Table I). For a transition of multipole order L , the K -hindrance factor f_ν , per degree of K -forbiddenness ν , where ν is

$$\nu = \Delta K - L,$$

can be expressed²⁸ as

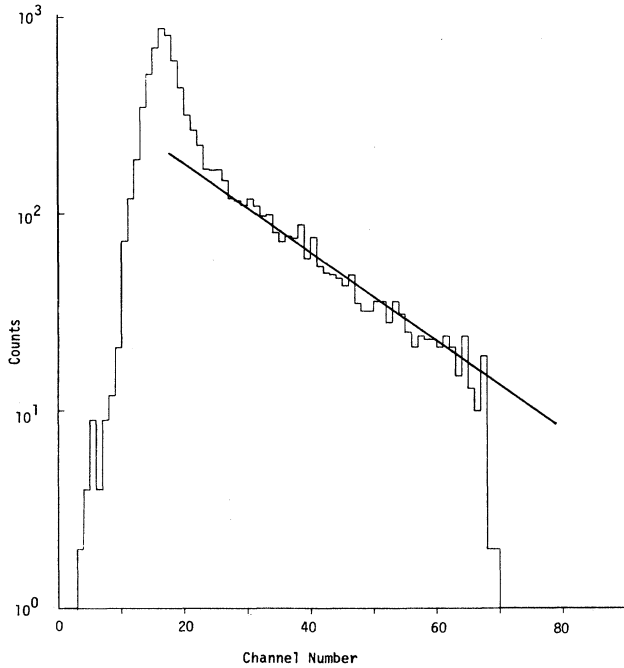


FIG. 9. TAC spectrum for 231-keV γ rays correlated with the β decay of $^{256}\text{Es}^m$. Detection of the β particle served as the start signal and the detection of the γ ray served as the stop signal. The straight line overlaying the data corresponds to a 70-ns half-life.

$$(f_\nu)^\nu = F_W .$$

For the 861.8- and 1092.9-keV transitions the degree of K -forbiddenness is $\nu=6$, giving f_ν values of 30.2 and 38.6, respectively. These values are comparable to the f_ν values of 26.0 and 31.6 for two $\Delta K=7$ $E1$ transitions of energy 671.1- and 1133.8-keV recently observed in ^{180}Os .²⁹ In both of these nuclei, above-average admixtures of lower K values in the $K^\pi=7^-$ state are presumed to be responsible for the low f_ν values. We note that the $\Delta K=5$, 380.0-keV $E2$ transition out of the 1425-keV level is also exceptionally fast ($F_W=1.4\times 10^4$, $f_\nu=25$). However, the hindrance factor for the 96.8-keV $\Delta K=2$, $E1$ transition ($F_W=8.2\times 10^6$) is not unusually low in comparison to those²⁷ of other $\Delta K=2$, $E1$ transitions.

C. Delayed fission results

We observed two delayed fissions which were time-correlated with the $^{256}\text{Es}^m$ β decay. Analysis of the data indicates that there is less than a 1% chance that these two events are due to random time correlations of unrelated β and fission events. The timing of the two fission events is consistent with decay from a state having a 70-ns half-life. This allows us to immediately rule out the 1560-keV level as the fissioning level, since fission from this level should be in prompt coincidence with the β de-

ay. Such prompt coincidences would be impossible to distinguish from coincidences arising from fission fragment conversion electrons. The delay of the two fissions, hence, requires the fissioning level to be either the 1425-keV level or a level fed by the 1425-keV level.

In our decay scheme, 100% of the $^{256}\text{Es}^m$ β decay passes through the 1425-keV level, either by direct feeding or via the 1560-keV level. If the delayed fissions arose from levels beneath the 1425-keV level, the delayed fission probability would be expressed as

$$P_{\text{DF}} = \frac{N_{\beta f}}{N_\beta B_\gamma} ,$$

where B_γ is the branching ratio describing feeding through the level of interest. Using the intensity scale in Table I, one can estimate B_γ for the lower-lying levels in ^{256}Fm . Using this method, we calculate P_{DF} values of 3.5×10^{-5} and 2.7×10^{-4} for the 563.7- and 1328.7-keV level, respectively. These levels are the most intense and highest-energy levels, respectively, populated from the 1425-keV delayed level. The 1425-keV level would have $P_{\text{DF}}=2\times 10^{-5}$. Using estimates for the γ lifetime of the lower levels on the order of 10–100 ps, we calculate partial fission half-lives on the order of 0.3–3 μs . If the fission lifetime were truly this short, one would expect fission from the 1425-keV level to have a comparable lifetime, if not shorter. This would mean fission from the 1425-keV level would proceed with a branching ratio of 0.02–0.2. Clearly, we do not observe that much fission from the 1425-keV level. Therefore, the fission lifetime must be longer than a few microseconds. With a longer fission half-life, fission from the picosecond levels below 1425-keV becomes essentially unobservable.

By this reasoning, we have assigned the fission activity to the 1425-keV level. This implies a fission half-life of $0.8_{-0.69}^{+8.8}$ ms at the 95% confidence level. The βDF probability was determined to be 2×10^{-5} relative to total β decay. This value is considerably lower than we had expected based on the original¹⁶ level scheme. The original level scheme, however, had not resolved the many levels between the 1425-keV level and the ground-state band which have been assigned in this work. The high admixture of these nearby levels reduces the half-life of the 1425-keV level considerably and hence reduces the branching ratio for fission from this level.

Using the 1425-keV level half-life and the estimate of ~ 2 μs for the unhindered fission half-life of this level,¹⁷ we calculate a hindrance for fission from this level of $\sim 10^3$. The magnitude of this hindrance factor is consistent with observed odd-particle fission hindrances³⁰ for ground-state fission from nuclei containing odd numbers of protons or neutrons. However, it is important to note that our experimentally observed hindrance factor is for an even-even nucleus in an excited state rather than its ground state. Presumably this excited state of fermion exists with two or more unpaired, or “odd,” nucleons and hence is a quasi-odd-odd nucleus, as one would expect if the 1425-keV state is truly analogous to the one predicted

by Soloviev and Siklos.²⁵

This result is important for attempts to produce heavier elements. Since spontaneous fission is expected to be the limiting factor to the stability of new elements, a reasonably high odd-particle hindrance at 1.4 MeV above the ground state of ^{256}Fm is encouraging for the existence of new longer-lived spontaneous fission isotopes and the continuing search for superheavy elements. Such hindrances enhance the survivability against fission of heavy nuclei formed in nuclear reactions, thus increasing the production yields. The increase, though modest, may be sufficient to increase production cross sections substantially.

Unfortunately, the low βDF probability resulting from hindered fission and the short γ half-life for the 1425-keV level preclude a study of the TKE and mass yields of fission from this excited-state. This information would have allowed some conclusions to be drawn about the nature of the fission process in a delayed fissile nucleus. No fission spectroscopy has yet been done on a delayed fission process, so there is no experimental information on the fission mechanism for the neutron-rich delayed fissile nuclei. Indeed, since the work of Baas-May¹⁰ has cast considerable doubt on the delayed fission decay of $^{236,238}\text{Pa}$ (Ref. 9), $^{256}\text{Es}^m$ is the only nuclide with an experimentally observed β -delayed fission branch.

Fission from the 1425-keV level in ^{256}Fm is also the first case in which fission has been observed from an isomeric state which is not in the second well of the potential energy surface. The very small fission branching ratio (2×10^{-5}) from the 1425-keV level strongly supports this being a level within the first well of the ^{256}Fm fission barrier. All theoretical studies of the potential energy surface in the heavy fermion region have resulted in the outer barrier being substantially smaller than the inner barrier. A level in the second well, i.e., a shape isomer, would decay predominantly by fission, not γ decay back to the ground state. The only observed fission to gamma ratio for a second-well isomer has been for $^{238}\text{U}^f$, where the barrier configuration is expected to favor γ deexcitation, and indeed a fission to gamma ratio of $4-5 \times 10^{-2}$ has been reported.³¹

IV. CONCLUSIONS

We have studied the decay of $^{256}\text{Es}^m$ isolated radiochemically from the $^{254}\text{Es}(t,p)$ reaction. Fifty-seven γ rays were assigned to 26 levels within the daughter ^{256}Fm , and an isomeric level at 1425 keV was seen. Fission was also observed from the 1425-keV level with a probability of 2×10^{-5} . The half-life of the 1425-keV level was determined to be 70 ± 5 ns and a partial fission half-life for this level was determined to be $0.8^{+8.8}_{-0.69}$ ms. Fission from this level, fed by the β decay of $^{256}\text{Es}^m$ constitutes β -delayed fission. From the fission to gamma ratio for deexcitation of the 1425-keV level, the 1425-keV level is assigned to be within the first minimum of the nuclear potential energy surface. This makes fission from the 1425-keV level the first observation of isomeric fission from within the first well of the potential energy surface, as well as the only observed βDF nucleus.

ACKNOWLEDGMENTS

This work was supported by the Director, Office of Energy Research, Division of Nuclear Physics of the Office of High Energy and Nuclear Physics of the U. S. Department of Energy under Contract Nos. DE-AC03-76SF00098 and W-7405-ENG-36. The authors are indebted (for the use of ^{254}Es) to the Division of Chemical Sciences, Office of Basic Energy Sciences, U. S. Department of Energy, through the transplutonium element production facilities at the Oak Ridge National Laboratory. This work was supported in part by a National Science Foundation Graduate Fellowship (H.L.H.). The results, views, and findings of this work are those of the authors only and do not necessarily reflect those of the National Science Foundation. The authors wish to thank the staff of the Los Alamos Ion Beam Facility for their invaluable assistance. Five of us (H.L.H., R.A.H., K.E.G., D.M.L., and D.C.H.) enjoyed the hospitality of the Isotope and Nuclear Chemistry Division of the Los Alamos National Laboratory during this experiment and wish to thank the INC Division. Many valuable discussions with Peter Möller concerning expected fission half-lives are gratefully acknowledged.

¹E. M. Burbidge, G. R. Burbidge, W. A. Fowler, and F. Hoyle, *Rev. Mod. Phys.* **29**, 547 (1957).

²J. Randrup, S. E. Larsson, P. Möller, A. Sobiczewski, and A. Lukasiak, *Physica Scr.*, **10A**, 60 (1974).

³H. V. Klapdor, C.-O. Wene, I. N. Isosimov, and Yu. W. Naumov, *Z. Phys. A* **292**, 249 (1979).

⁴Yu. A. Lazarev, Yu. Ts. Oganessian, and V. I. Kuznetsov, Joint Institute for Nuclear Research Report No. JINR-E7-80-719 (1980).

⁵H. V. Klapdor, T. Oda, J. Metzinger, W. Hillebrandt, and F. K. Thielman, *Z. Phys. A* **299**, 213 (1981).

⁶C.-O. Wene and S. A. E. Johansson, *Phys. Scr.* **10A**, 156 (1974).

⁷R. W. Hoff, Lawrence Livermore National Laboratory Report No. UCRL-94252 (1986).

⁸R. W. Hoff, Lawrence Livermore National Laboratory Report No. UCRL-97056 (1988).

⁹Yu. P. Gangrskii, G. M. Marinescu, M. B. Miller, V. N. Samoyusk, and I. F. Kharisov, *Yad. Fiz.* **27**, 894 (1978) [*Sov.*

J. Nucl. Phys. **27**(4), 475 (1978)].

¹⁰A. Baas-May, J. V. Kratz, and N. Trautmann, *Z. Phys. A* **322**, 457 (1985).

¹¹V. I. Kuznetsov, N. K. Skobelev, and G. N. Flerov, *Yad. Fiz.* **5**, 271 (1966) [*Sov. J. Nucl. Phys.* **5**, 191 (1966)].

¹²N. K. Skobelev, *Yad. Fiz.* **15**, 444 (1972) [*Sov. J. Nucl. Phys.* **15**, 249 (1972)].

¹³D. Habs, H. Klewe-Nebenius, V. Metag, B. Neumann, and H. J. Specht, *Z. Phys. A* **285**, 53 (1978).

¹⁴R. Hingman, W. Kuehn, V. Metag, R. Novotny, A. Ruckelshausen, H. Stroehrer, F. Hessberger, S. Hofmann, G. Muenzenberger, and W. Reisdorf, Gesellschaft für Schwerionenforschung Darmstadt Report No. GSI 85-1, 88 (1985).

¹⁵Yu. A. Lazarev, Yu. Ts. Oganessian, I. V. Shirokovsky, S. P. Tretyakova, V. K. Utyonkov, and G. V. Buklanov, *Europhys. Lett.*, **4**, 893 (1987).

¹⁶R. W. Loughheed, J. H. Landrum, D. C. Hoffman, W. R. Daniels, J. B. Wilhelmy, M. E. Bunker, J. W. Starner, and S.

- V. Jackson, *Proceedings of the 3rd International Conference on Nuclei Far From Stability, Cargese, Corsica, 1976* (CERN, Geneva, 1976).
- ¹⁷P. Möller (private communication).
- ¹⁸H. L. Smith and D. C. Hoffman, *J. Inorg. Nucl. Chem.* **3**, 243 (1956).
- ¹⁹G. R. Choppin and R. J. Silva, *J. Inorg. Nucl. Chem.* **3**, 153 (1956).
- ²⁰E. P. Horowitz, C. A. A. Bloomquist, and D. J. Henderson, *J. Inorg. Nucl. Chem.* **31**, 1149 (1969).
- ²¹E. P. Horowitz and C. A. A. Bloomquist, *Inorg. Nucl. Chem. Letters* **5**, 753 (1969).
- ²²E. P. Horowitz and C. A. A. Bloomquist, *J. Inorg. Nucl. Chem.* **34**, 3851 (1972).
- ²³I. Ahmad, H. Diamond, J. Milsted, J. Lerner, and R. K. Sjoblom, *Nucl. Phys.* **A208**, 287 (1973).
- ²⁴P. H. Stelson, R. W. Lide, and C. R. Bingham, *Nucl. Phys.* **A144**, 254 (1970).
- ²⁵V. G. Soloviev and T. Siklos, *Nucl. Phys.* **59**, 145 (1964).
- ²⁶K. Neergård and P. Vogel, *Nucl. Phys.* **A149**, 217 (1970).
- ²⁷K. E. G. Löbner, *Phys. Lett.* **26B**, 369 (1968).
- ²⁸J. Borggreen, N. J. S. Hansen, J. Pederson, L. Westgaard, J. Zylicz, and S. Bjornholm, *Nucl. Phys.* **A96**, 561 (1967).
- ²⁹R. M. Lieder, and A. Neskakis, J. Skalski, G. Sletten, J. D. Garrett, and J. Dudek, *Nucl. Phys.* **A476**, 545 (1988).
- ³⁰D. C. Hoffman and L. P. Somerville, *Charged Particle Emission from Nuclei Vol. III* (CRC Press, Boca Raton, FL., in press); also, Lawrence Berkley Laboratory Report No. LBL-23475.
- ³¹P. A. Russo, J. Pedersen, and R. Vandenbosch, *Proceedings of the Third International Symposium on Physics and Chemistry of Fission (Rochester, New York, 1973)* (International Atomic Energy Agency, Vienna, 1974), p. 271.